OPEN ACCESS Science International

ISSN 2305-1884
DOI: 10.17311/sciintl.2018.31.38

Research Article
Leaching Behaviour of Some Hazardous Metals from Radiated Exhausted and Metal-doping Stannic Antimonate Materials

Mamdouh Mohamed Abou-Mesalam, Asmaa Bendary Ibrahim and Moustafa Mohamed El-Shorbagy

Atomic Energy Authority, Hot Labs. Centre, P.Code13759, Cairo, Egypt

Abstract

Objective: The objective was to study the leaching behavior of Co^{2+} and Cd^{2+} ions from stannic antimonate, cobalt and strontium doped stannic antimonate at different conditions. **Methodology:** The total capacity of stannic antimonate and its dopants cobalt and strontium stannic antimonates for Co^{2+} and Cd^{2+} ions were investigated before and after irradiated at different doses. The crystallite size and lattice strain of stannic antimonate and its dopants cobalt and strontium stannic antimonates after saturation with Co^{2+} and Cd^{2+} ions were determined at different irradiation doses. The surface area values of stannic antimonates and its dopants were measured using BET-technique. **Results:** The leach rate values of Co^{2+} ion from stannic antimonate saturated with cobalt and cobalt stannic antimonate at different irradiation doses were determined and show the leach rate values of Co^{2+} ion from cobalt stannic antimonate lower than those obtained from stannic antimonate saturated with cobalt. **Conclusion:** The leach rate of ion was decreased by doping of the same ion with the ion exchanger and increasing the radiation dose that exposed to the exchange materials from 0-100 kGy.

Key words: Stannic antimonate, doping, inorganic ion exchanger, crystallite size, lattice strain, leachability

Citation: Mamdouh Mohamed Abou-Mesalam, Asmaa Bendary Ibrahim and Moustafa Mohamed El-Shorbagy, 2018. Leaching behaviour of some hazardous metals from radiated exhausted and metal-doping stannic antimonate materials. Sci. Int., 6: 31-38.

Corresponding Author: Mamdouh Mohamed Abou-Mesalam, Atomic Energy Authority, Hot Labs. Centre, P.Code13759, Cairo, Egypt Tel: 00201224506010

Competing Interest: The authors have declared that no competing interest exists.

Data Availability: All relevant data are within the paper and its supporting information files.

INTRODUCTION

Powder X-ray diffraction analysis is useful for many purposes, such as structure determination, phase identification and quantification in solid mixtures, estimate of preferred orientation effects, lattice micro strain and mean crystallite size[1-5]. Furthermore, powder diffraction techniques do not need prior hard steps of sample preparation. For instance, sometimes only grinding procedures were enough to avoid preferred orientation of crystallites. The two main properties extracted from peak width analysis were (a) Crystallite size and (b) Lattice strain. Crystallite size is a measure of the size of a coherently diffracting domain. The crystallite size of the particles was not generally the same as the particle size due to the presence of polycrystalline aggregates[6]. The most common techniques used for the measurement of particle size rather than the crystallite size are BET, light scattering, scanning electron microscopy and transmission electron microscopy (TEM) analysis. Lattice strain is a measure of the distribution of lattice constants arising from crystal imperfections, such as lattice dislocation. The other sources of strain are the grain boundary triple junction, contact or sinter stresses, stacking faults, coherency stresses, etc.[7]. In previous publications a new category of inorganic materials was synthesized such as silico-antimonate[8], uranium antimonate[9] and vanadium antimonate[10]. The aim of this study was to estimate the crystallite size and lattice strain of stannic antimonate and its dopants cobalt stannic antimonate and strontium stannic antimonate after saturation with cobalt and strontium, also studied the leaching rates of these ion exchangers in different media.

MATERIALS AND METHODS

Chemicals and reagents: All chemicals and reagents were of analytical grade purity and used without further purification.

Synthesis of stannic-antimonate (SnSb) ion exchanger: Stannic-antimonate was synthesized by the reaction of 0.1 M stannic tetra chloride (dissolved in distilled water) with 0.1 M antimony metal (dissolved in aqua regia) with molar ratio Sn to Sb equal 1:1. During the addition process, yellow gelatinous precipitates were formed. After complete addition, few drops of diluted ammonia solution were added for complete precipitation, the precipitate left overnight standing and the mixture was hydrolyzed in distilled water and left for 2 days at room temperature. The precipitate formed was separated by centrifugation at 3000 rpm for 5 min. The precipitate was washed by 0.1 M HNO_3 to be free from Cl^- ions and rewashed by distilled water to remove NO_3^-. The precipitate was dried at 60 °C in a drying oven and washed with hot water (70°C) to remove the air traps in the solid and then redried at 60°C. The solid was ground, sieved to mesh size and stored at room temperature.

Synthesis of doping cobalt or strontium stannic antimonate (CoSnSb or SrSnSb) ion exchangers: Cobalt or strontium chloride solutions with concentration of 0.1 M were used for doped cobalt or strontium *in-situ* stannic-antimonates. Cobalt or strontium stannic-antimonate solid samples were prepared by the reaction of 0.1 M cobalt chloride or 0.1 M strontium chloride with a mixture of 0.1 M stannic tetra chloride (dissolved in distilled water) and 0.1 M antimony metal (dissolved in aqua regia) with volumetric molar ratio equal to unity (Co/or Sr:Sn:Sb equal 1:1:1). The reaction carried out in water bath at 60°C with continuous stirring for 4 h. Greenish yellow gelatinous or reddish gelatinous precipitate for CoSnSb or SrSnSb formed during the addition process of cobalt chloride or strontium chloride, respectively, to the mixture. After an overnight standing the precipitate separated by centrifugation at 3000 rpm. The solids treated by 0.1 M HNO_3 to remove impurities and Cl^- ions. Solids rewashed with distilled water to remove NO_3^- ions. After drying in drying oven at 60°C, the granules solids were poured in near boiling water at 70-80°C to remove the trapped air. Dry, grand, sieve and store solids at room temperature.

Surface area measurements: The surface area values of stannic antimonate saturated with cobalt and cobalt stannic antimonate were measured using BET-technique as adsorption phenomena of nitrogen gas on the powder surface at 77 K.

X- ray diffraction patterns: Powder X-ray diffraction was performed using a Shimadzu X-ray diffractometer, model XD610, with a nickel filter and Cu-K_α radiation (1.54 A°) operating at 30 kV and 30 mA.

Capacity measurements: The capacity of synthesized stannic antimonate saturated with cobalt and cobalt stannic antimonate for Co^{2+} and Cd^{2+} ions were determined by the

repeated batch technique, by equilibrating nearly 0.7 g of stannic antimonate and doping stannic antimonate with 70 mL of (30 ppm) Co^{2+} and Cd^{2+} ion solutions on a shaker thermostat adjusted at 25±1°C. After equilibrium, the solution was separated and repeated until no further sorption occurs. The capacity was calculated using the Eq. 1:

$$\text{Capacity in (mg g}^{-1}) = \%\frac{\text{Uptake}}{100}\times\frac{v}{m}\times C_O \quad (1)$$

$$\%\text{Uptake} = \frac{A_O - A}{A_O}\times 100 \quad (2)$$

Where:

A_o and A = The initial and final concentration of ions of solution

C_o = The initial concentration of solution

V = The solution volume (mL)

m = The weight of the exchanger (g)

Static leaching tests: In static leach tests, stannic antimonate saturated with cobalt and cobalt stannic antimonate samples (dried at 50°C) were used to obtain the leach rates of co^{2+} ion in different media. The experiments were carried out by mixing 0.1 g of stannic antimonate saturated with cobalt and cobalt stannic antimonate with 10 mL of the leachate solutions (dist. H_2O, 0.1 M HNO_3 and 0.5 M HNO_3) at 25±1°C in absence of stirring. After an equilibrium, the solution was separated and repeated until no further desorption occurs. The liquid samples were analyzed for the leached Co^{2+} ion content . The leaching rates of the corresponding cations were calculated according to the following equation:

$$\text{Leach rate} = \frac{A}{A_o}\cdot\frac{W}{(S.T)}\text{g cm}^{-2}\text{.d} \quad (3)$$

Where:

A = The amount of ions leached out from the sample in unit time (T)

A_o = The amount of ions loaded on stannic antimonate

W = The mass (g) of the sample used in the test and

S = The surface area (cm^2) of the sample determined by nitrogen adsorption method

RESULTS AND DISCUSSION

X-ray diffraction analysis: The XRD patterns of synthesized stannic antimonate and doping Co^{2+} and Sr^{2+} stannic antimonate samples after saturation with Co^{2+} and Cd^{2+} ions show crystalline nature as showed in Fig. 1(a-f). The peaks intensity was sharp and narrow, confirming that the samples were of high quality with good crystallinity. Using XRD data, lattice parameters were calculated (a = 3.2491 Å and c = 5.2063 Å). The data in Fig. 1 (a-f) show different peaks at different 2θ with variable intensities indicating the crystalline nature of these materials. The brag angle 2θ and the full width at half maximum (β) were determined to evaluate the crystallite size and lattice strain of these materials.

From Debye-Scherrer's formula:

$$D = \frac{K.\lambda}{\beta.\text{Cos}\theta} \quad (4)$$

Where:

D = The effective average crystalline size

K = The shape factor (0.89)

λ = The wavelength of CuKα radiation in nanometer

θ = The Bragg diffraction angle and

β = The measured full width at half maximum (FWHM)

The lattice strain induced in powders due to crystal imperfection and distortion was calculated using Hall equation with the formula[11-13]:

$$\frac{\beta.\cos\theta}{\lambda} = \frac{1}{D} + \frac{(\varepsilon.\text{in}\theta)}{\lambda} \quad (5)$$

where, ε is the effective strain. By substitution in Eq. 5 from 4 about the value of (ε) Eq. 4 becomes:

$$\frac{\beta.\cos\theta}{\lambda} = \frac{\beta.\cos\theta}{K.\lambda} + \frac{(\varepsilon.\sin\theta)}{\lambda} \quad (6)$$

By multiplying both sides of Eq. 6 in constant value {λ/(β.Cosθ)} and after rearranging the equation is:

$$\varepsilon = \frac{\beta}{4\text{Tan}\theta} \quad (7)$$

From Eq. 4 and 6, it was confirmed that the peak width from crystallite size varies as 1/Cos θ strain varies as tan θ.

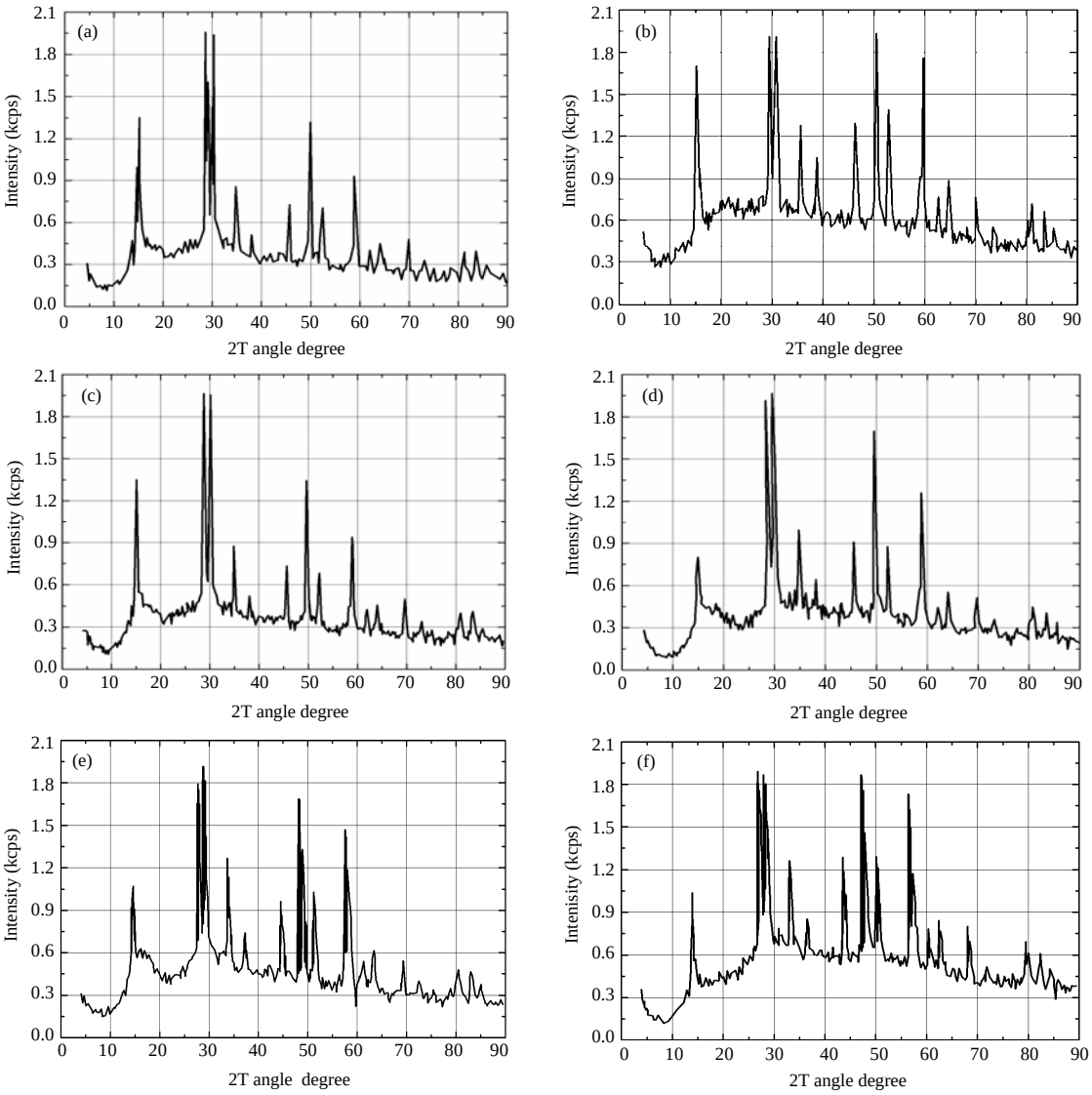

Fig. 1(a-f): (a)XRD of SnSb (0) after saturation by cadmium ion, (b) XRD of SnSb (0) after saturation by cobalt, (c) XRD of CoSnSb (0) after saturation by cadmium ion, (d) XRD of CoSnSb (0) after saturation by cobalt ion, (e) XRD of SrSnSb (0) after saturation by cadmium ion and (f) XRD of SrSnSb (0) after saturation by cobalt ion

Assuming that the particle size and strain contributions to line broadening are independent to each other and both have a Cauchy-like profile, the observed line breadth is simply the sum of Eq. 4 and 7:

$$\beta = \{K \cdot \lambda / D \cos\theta\} + 4\varepsilon \tan\theta \quad (8)$$

By rearranging the above Eq. get the:

$$\beta.\cos\theta = \{K.\lambda/D\} + 4\varepsilon \sin\theta \quad (9)$$

The above equations are Williamson-Hall's (W-H) equations.

By plotting of the relation between (4 Sinθ) along the x-axis and (β.Cosθ) along the y-axis, the crystallite size and the lattice strain (ε) were estimated from the y-intercept and the slope of the fit, respectively and the results were represented in Table 1 and 2. From data in Table 1 and 2 crystallite size of cobalt stannic antimonate and strontium stannic antimonate are higher those of stannic antimonate that may be related to doping in-situ precipitation of cobalt and strontium with stannic antimonate. From the data in Table 1 and 2 the crystallite size of SnSb and doping CoSnSb and SrSnSb saturated by Cd^{2+} ion was found. This may be due to the higher complexbility of Co^{2+} ion compared to Cd^{2+} ion that leads to strain in the crystallite size of SnSb and CoSnSb and

Table 1: Crystallite size and lattice strain for stannic antimonate and doping stannic antimonate after saturation by Cd^{2+} ion

Ion exchanger	Dose (kGy)	D (Crystallite size, nm) × 10^{-2}	Lattice strain (ε)
SnSb	0	13.05	0.178
	10	14.27	0.166
	50	16.17	0.1415
	100	17.34	0.096
CoSnSb	0	14.12	0.172
	10	17.80	0.157
	50	19.03	0.087
	100	20.15	0.059
SrSnSb	0	14.73	0.200
	10	15.70	0.166
	50	16.51	0.140
	100	17.13	0.158

SnSb: Stannic-antimonate, CoSnSb: Cobalt stannic-antimonate, SrSnSb: Strontium stannic-antimonate

Table 2: Crystallite size and lattice strain for stannic antimonate and doping stannic antimonate after saturation by Co^{2+} ion

Ion exchanger	Dose (kGy)	D (Crystallite size, nm) × 10^{-2}	Lattice strain (ε)
SnSb	0	11.91	0.3703
	10	13.05	0.172
	50	14.12	0.166
	100	14.73	0.125
CoSnSb	0	13.43	0.2272
	10	14.12	0.214
	50	15.75	0.140
	100	17.80	0.100
SrSnSb	0	14.27	1.250
	10	14.89	0.180
	50	15.75	0.170
	100	17.13	0.208

SnSb: Stannic-antimonate, CoSnSb: Cobalt stannic-antimonate, SrSnSb: Strontium stannic-antimonate

Table 3: Leaching rate of Co^{2+} ion from unirradiated and irradiated saturated SnSb and doped Co-SnSb ion exchange materials

		Leach rate, cm^2/d		
Ion exchangers	Dose (kGy)	Distilled H_2O	0.1 M HNO_3	0.5 M HNO_3
Saturated SnSb by Co^{2+}	0	1.40	7.2	9.8
	10	0.02	2.8	3.9
	50	0.01	2.4	4.9
	100	0.01	2.1	4.01
Doped saturated CoSnSb	0	0.03	3.9	7.1
	10	0.02	2.1	2.3
	50	0.01	1.4	1.6
	100	0.02	0.7	0.8

SnSb: Stannic-antimonate, CoSnSb: Cobalt stannic-antimonate, SrSnSb: Strontium stannic-antimonate

SrSnSb. Also, Table 1 and 2 showed that the strain in samples saturated by Cd^{2+} ion was higher than those of samples saturated by Co^{2+} ion. Also Table 1 and 2 indicated that the strain in ion exchangers decreases as the crystallite size increased which was unusual phenomena[14,15]. Owing to the large number of grain boundaries and the short distance between them, the intrinsic strain associated with such interface are always present in nano-and crystallite structural materials.

Surface area measurement: The surface area values of stannic antimonate saturated with cobalt and doping cobalt stannic antimonate were found to be 36.28 and 53.51 $cm^2 g^{-1}$, respectively, as determined by the BET adsorption of nitrogen gas. The surface area of doping cobalt stannic antimonate sample was increased from 36.28-53.51 cm^2 g^{-1}. These increasing in the surface area values may be due to the bond formation of the doped Co^{2+} ion with tin and antimony atoms during the preparation process that leading to an increase in the structure chain of the exchanger.

Leaching rates of Co^{2+}: Static leaching rate of Co^{2+} ion and doped Co-stannic antimonate were investigated in different media such as distilled water, 0.1 M HNO_3 and 0.5 M HNO_3. The static batch test was carried out for along 4 days and the data were represented in Table 3 and Fig. 2(a-h). Generally, from Fig. 2(a-h) the leach rate of Co^{2+} ion in distilled water medium was lower than that obtained in nitric acid media.

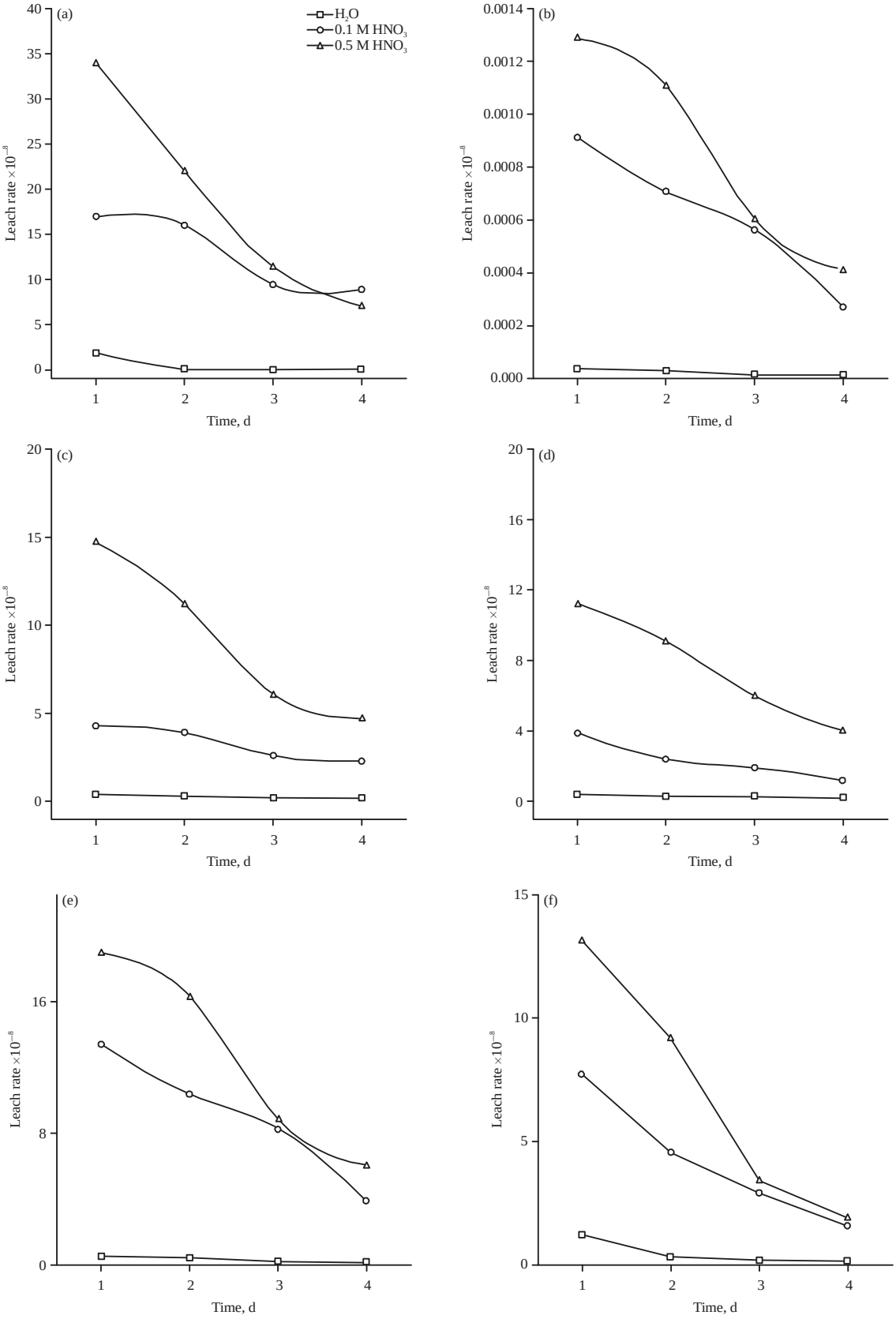

Fig. 2(a-h): continue

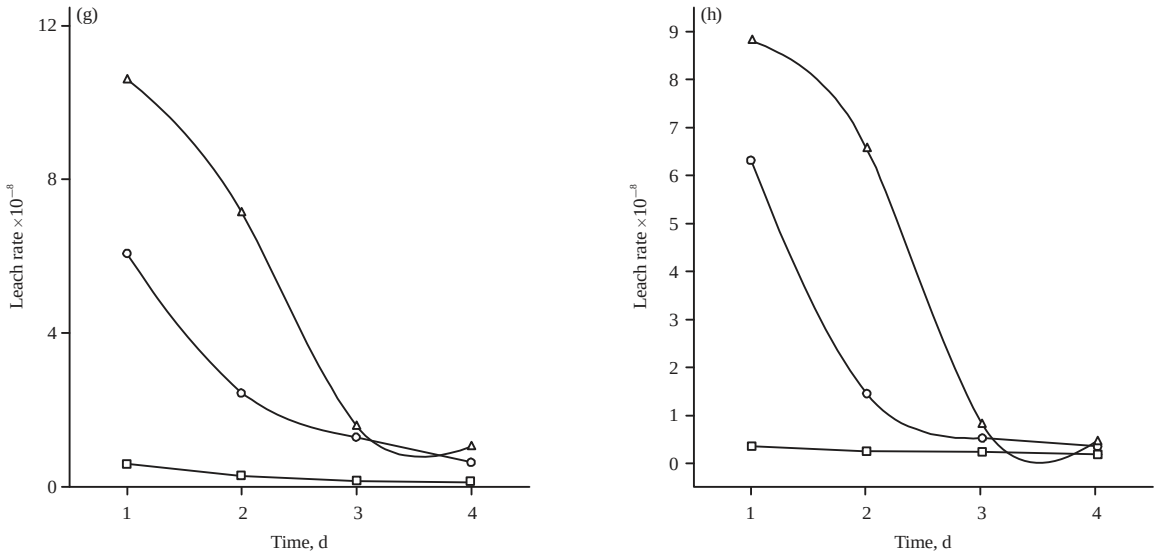

Fig. 2(a-h): (a) Leach rate of Co^{2+} ion from stannic antimonate saturated with cobalt as a function of time at 0 radiation, (b) Leach rate of Co^{2+} ion from stannic antimonate saturated with cobalt as a function of time at 10 kGy radiation, (c) Leach rate of Co^{2+} ion from stannic antimonate saturated with cobalt as a function of time at 50 kGy radiation, (d) Leach rate of Co^{2+} ion from stannic antimonate saturated with cobalt as a function of time at 100 kGy radiation, (e) Leach rate of Co^{2+} ion from cobalt stannic antimonate as a function of time at 0 radiation, (f) Leach rate of Co^{2+} ion from cobalt stannic antimonate as a function of time at 10 kGy radiation, (g) Leach rate of Co^{2+} ion from cobalt stannic antimonate as a function of time at 50 kGy radiation and (h) Leach rate of Co^{2+} ion from cobalt stannic antimonate as a function of time at 100 kGy radiation

The data in Fig. 2(a-h) indicated that the leach rate of Co^{2+} ion from stannic antimonate saturated by Co^{2+} (Fig. 2a-d) and doped Co-stannic antimonate (Fig. 2e-h) were decreased by increasing the radiation dose that exposed to the exchange materials from 0-100 kGy. This may be attributed to the collapse of the surface of stannic antimonate at high radiation dose and Co^{2+} ion is trapped in the cavities and channels of the exchange material[16]. This means that the radiation treatment led to further improvement in the leach resistance of the leaching ion from stannic antimonate. By the comparison of data from Fig. 2(a-h) found that the leaching rate of Co^{2+} ion from doped Co-stannic antimonate samples are very low compared to these obtained from stannic antimonate saturated by cobalt samples. This behaviour may be related to building nature of Co^{2+} ion in the texture of the materials. Finally Table (3) summarized the leaching rate of Co^{2+} ion from saturated SnSb by Co^{2+} ion and doped Co-SnSb after 4 days for unirradiated and irradiated materials.

CONCLUSION

The leach rate values of Co^{2+} ion from stannic antimonate saturated with cobalt and cobalt stannic antimonate at different irradiation doses were determined and show the leach rate values of Co^{2+} ion from cobalt stannic antimonate lower than those obtained from stannic antimonate saturated with cobalt. The leach rate of ion was decreased with increasing the radiation dose that exposed to the exchange materials from 0-100 kGy.

SIGNIFICANCE STATEMENT

This study for the first time conduct the effect of gamma radiation on the leaching behavior of some hazardous ions such as Co^{2+} ion from doped and undoped ion exchange materials in different media.

REFERENCES

1. Nemet, Z., G.C. Kis, G. Pokol and A. Demeter, 2009. Quantitative determination of famotidine polymorphs: X-ray powder diffractometric and Raman spectrometric study. J. Pharm. Biomed. Anal., 49: 338-346.
2. Pecharsky, V. and P. Zavalij, 2009. The Powder Diffraction Pattern. In: Fundamentals of Powder Diffraction and Structural Characterization of Materials, Pecharsky, V. and P. Zavalij (Eds.). 2nd Edn., Springer, New York, ISBN: 9780387095783, pp: 151-201.

3. Giacovazzo, C., H.L. Monaco, G. Artioli, D. Viterbo and M. Milanesio *et al.*, 2011. Fundamentals of Crystallography. 3rd Edn., Oxford University Press, Oxford.
4. Jenkins, R. and R.L. Snyder, 1996. Introduction to X-Ray Powder Diffractometry. Wiley, New York.
5. Young, R.A., 1993. The Rietveld Method. Oxford University Press, New York.
6. Hebbar, K.R., 2007. Basics of X-ray Diffraction and its Application. I.K. International Publishing House Pvt. Ltd., New Delhi, ISBN: 9788189866075, Pages: 272.
7. Ungar, T., 2007. Characterization of nanocrystalline materials by X-ray line profile analysis. J. Mater. Sci., 42: 1584-1593.
8. Abou-Mesalam, M.M., 2003. Sorption kinetics of copper, zinc, cadmium and nickel ions on synthesized silico-antimonate ion exchanger. Colloids Surf. A: Physicochem. Eng. Aspects, 225: 85-94.
9. Sivaiah, M.V., K.A. Venkatesan, R.M. Krishna, P. Sasidhar and G.S. Murthy, 2004. Ion exchange studies of europium on uranium antimonate. Colloids Surfaces A: Physicochem. Eng. Aspects, 236: 147-157.
10. Morales, J., L. Sanchez, F. Martin and F. Berry, 2006. Electrochemical reaction of lithium with nanosized vanadium antimonate. J. Solid State Chem., 179: 2554-2561.
11. Gu, F., S.F. Wang, M.K. Lu, G.J. Zhou, D. Xu and D.R. Yuan, 2004. Structure evaluation and highly enhanced luminescence of Dy^{3+}-doped ZnO nanocrystals by Li^{+} doping via combustion method. Langmuir, 20: 3528-3531.
12. Cullity, B.D. and S.R. Stock, 2001. Elements of X-ray Diffraction. 3rd Edn., Prentice Hall, New Jersey, ISBN: 0201610914, Pages: 664.
13. Abou-Mesalam, M. and I. El-Naggar, 2009. Chemical deposition of zirconium doped tin silicate ion-exchanger and its characterization. J. Radioanal. Nucl. Chem., 279: 333-340.
14. Abou-Mesalam, M.M., 2013. Evaluation of crystallite size and lattice strain in nano particles of transition metals hexacyano ferrate. Int. J. Adv. Chem. Technol., 2: 13-18.
15. Edelstein, A.S. and R.C. Cammaratra, 1998. Nanomaterials: Synthesis, Properties and Application. 2nd Edn., CRC Press, USA., ISBN: 9780750305785, pp: 214-241.
16. Abou-Mesalam, M.M. and I.M. El-Naggar, 2002. Applications of inorganic ion exchangers: I-sorption and fixation of some radionuclides in synthetic iron (III) titanate ion exchanger. Arab J. Nucl. Sci. Applic., 35: 95-105.